JMEPEG (2010) 19:928–935
DOI: 10.1007/s11665-009-9561-0

1059-9495/$19.00

Inverse Analysis of Rapid and Localized Energy Deposition

S.G. Lambrakos and J.G. Michopoulos

(Submitted July 13, 2009)

This paper examines multiscale inverse analysis of rapid and localized energy deposition, where there exists extremely strong filtering of spatial and temporal structure within the associated diffusion pattern. This strong filtering tends to establish conditions where system identification, or in particular reconstruction of detailed features of the energy source, based on data-driven inverse analysis of the diffusion pattern alone is not well posed. An accurate and well-posed characterization of rapid energy deposition processes should be in terms of two distinctly separate scales for both spatial and temporal structures. Accordingly, the inverse rapid and localized energy deposition problem requires a formulation with respect to system identification and parameterization that should be cast in terms of two separate sets of parameters. One should represent energy source characteristics on spatial and temporal scales commensurate with that of thermal diffusivity within the material. The other parameter set should represent energy source characteristics on spatial and temporal scales commensurate with those of surface phenomena. The general procedure presented here for inverse analysis of rapid and localized energy deposition is formulated in terms of these two separate sets of parameters.

Keywords filtering, heat deposition, inverse problems, multiscale

1. Introduction

The issues examined here concern inverse analysis of energy deposition in metals under conditions of extremely rapid relative motion and spatial localization of the energy source with respect to surfaces of structures, with potential applications to the analysis of systems characterized by sliding surfaces that are in contact. That is to say, applications having deposition speeds that are comparable to and in excess of those of deep penetration welding processes and yet have highly localized coupling of energy at surfaces. The inverse energy deposition problem represents a particular subclass of the more general inverse heat conduction problem (Ref 1-4), where certain characteristic trend features that are associated with the diffusion pattern dominate (Ref 5, 6). For energy deposition processes where the rates of deposition and of surface coupling of energy are moderate, such as in welding processes, inverse analysis has been successfully applied for system identification and parameterization. In the case of very rapid and spatially localized energy deposition, however, there exists extremely strong filtering of spatial and temporal structure within the associated diffusion pattern. This strong filtering tends to establish conditions where system identification, or in particular reconstruction of detailed features of the energy source, based on data-driven inverse analysis of spatial and temporal structure within the temperature field diffusion pattern is not well posed. Accordingly, the inherent nature of rapid and localized heat deposition requires that the interpretation of sensor data be based on multiscale paradigms, which are in terms of both time and space.

This goal is achieved in this study, by the formulation of a general approach for multiscale inverse analysis of rapid and localized energy deposition, where there exists extremely strong filtering of spatial and temporal structure within the associated diffusion pattern. Methods of inverse analysis (Ref 7, 8), in contrast to analysis methods based on the direct-problem approach (i.e., methods that are model-driven only), are characterized by many properties that follow directly from the fact that inverse methods are data driven as well as model driven. Among these properties is that relatively complex and highly nonlinear systems can be represented accurately by means of model representations characterized by small numbers of parameters. In many cases, the errors that are introduced by approximations underlying an inverse model, and its relatively minimal parameterization, are in fact compensated for by the characteristics of the data space. In that the data space determines those models within model space that are potentially applicable for inverse analysis, it remains an open question as to what should be the potential composition of the data space for very rapid and highly localized energy deposition, i.e., what measurements are possible and accordingly of significance for system identification.

In this work, a statement of the specific multiscale inverse problem to be considered is presented, as well as a general approach for multiscale inverse analysis of rapid and localized energy deposition. The multiscale nature of rapid and localized energy deposition follows from a natural partitioning of scale regimes that results from the filtering properties of the heat conduction kernel. Physical assumptions and mathematical

S.G. Lambrakos and **J.G. Michopoulos**, Computational Multiphysics Systems Laboratory, Code 6394, Center for Computational Material Science, U.S. Naval Research Laboratory, Washington, DC 20375. Contact e-mail: lambrakos@anvil.nrl.navy.mil.

approximations underlying this analysis are elucidated. A description is then presented of prototype data that is adopted for inverse analysis and of the numerical model that is used for its generation. Subsequently, prototype inverse analyses are applied to prototype data for the purpose of examining the general posedness of this approach.

2. Statement of Inverse Problem

The inverse problem concerning analysis of physical processes, in general (Ref 9), and the inverse heat transfer problem, in particular (Ref 10), may be stated formally in terms of source functions (or input quantities) and multidimensional fields (output quantities). Considered here, however, is a restricted class of inverse heat transfer problems. This restricted class is that of the inverse analysis of heat deposition processes where the rate of deposition is extremely rapid, and the quantities are those that characterize the source function $q(x, y, z, t)$ in terms of its volumetric spatial and temporal characteristics, either locally or at accessible locations on the boundary of a workpiece structure. The data space for analysis of this system will in general consist of (a) measurements of the temperature $T(x, y, z, t)$ at different locations and times on the boundary surfaces of the spatial region of interest, e.g., thermocouple measurements, (b) the location of the central point of the source function $q(x, y, z, t)$ within the volume of the region of interest, e.g., post-mortem melting or solid-state transformation profiles on the metal surface, (c) information concerning the spatial and temporal characteristics of the source function $q(x, y, z, t)$, and (d) information concerning the thermal diffusivity of the material making up the structure. Information concerning the spatial and temporal characteristics of $q(x, y, z, t)$ would include the shapes of solidification boundaries resulting from localized melting. Information concerning the thermal diffusivity of the material would be the average diffusivity for a range of temperatures. The precise mathematical statement of the inverse problem considered here, and the general methodology for its solution (Ref 6, 11), are defined according to the fact that in general a heat conductive system occupying an open-bounded domain Ω with an outer boundary Γ_o and an inner boundary Γ_i involves the parabolic equation

$$\frac{\partial T(\hat{x},t)}{\partial t} = \nabla \cdot (\kappa(\hat{x},t)\nabla T(\hat{x},t)) \quad \text{in } \Omega \times (0,t_f), \qquad \text{(Eq 1a)}$$

with initial condition

$$T(\hat{x},0) = T_0(\hat{x}) \text{ in } \Omega, \qquad \text{(Eq 1b)}$$

and heat flux exchanges through the outer and inner boundaries Γ_o and Γ_i as follows:

$$-\kappa(\hat{x},t)\frac{\partial T(\hat{x},t)}{\partial n_{\Gamma_o}} = c(\hat{x},t)(T(\hat{x},t) - T_a(\hat{x},t)) \quad \text{on } \Gamma_0 \times (0,t_f), \qquad \text{(Eq 1c)}$$

$$-\kappa(\hat{x},t)\frac{\partial T(\hat{x},t)}{\partial n_{\Gamma_i}} = q(\hat{x},t) \quad \text{on } \Gamma_i \times (0,t_f). \qquad \text{(Eq 1d)}$$

Here $\hat{x} = (x,y,z)$ is the position vector, n_{Γ_o} and n_{Γ_i} are the normal vectors onto boundaries Γ_o and Γ_i, respectively, t is the time variable, t_f is the final time, $T(\hat{x},t) = T(x,y,z,t)$ is the temperature field variable, $\kappa(\hat{x},t) = \kappa(x,y,z,t)$ is the heat conductivity field variable, $c(\hat{x},t) = c(x,y,z,t)$ and $T_a(\hat{x},t) = T_a(x,y,z,t)$ are specified functions, and $q(\hat{x},t) = q(x,y,z,t)$ is the heat flux on the inner boundary Γ_i. Determination of the temperature field via solution of Eq 1(a-d) constitutes the so-called forward or direct initial-boundary value problem. The interest here, however, is focused on a specific formulation of the inverse problem. This formulation entails essentially reconstruction of the heat flux field $q(x, y, z, t)$ on the inner boundary Γ_i, and the resulting temperature field $T(x, y, z, t)$ for all time $t \in [0, t_f]$ when Γ_i is totally or partially inaccessible. In order to reconstruct the heat flux, some extra information concerning the temperature $T(x, y, z, t)$ is needed (i.e., known values experimentally acquired).

At this stage, it is illuminating to comment on general conditions for which the inverse heat transfer problem is well posed. First, as is well known, the inverse heat transfer problem as defined such that one seeks information concerning the source function from measurements of the temperature field is not well posed for all conditions. The inverse heat deposition problem, however, as defined according to Eq 1(a) to (d), is well posed for a wide range of conditions, especially those typical of most practical applications such as welding and heat treatment. As demonstrated previously (Ref 12), as a consequence of filtering properties, the inverse heat deposition problem under conditions of rapid deposition is not well posed unless it is defined with respect to two separate scales for space and time. That is to say, the inverse rapid heat deposition problem is well posed as defined according to Eq 1(a) to (d) with respect to multiple scales, i.e., separate space and time scales for the two different regions specified by their proximity to the boundaries Γ_o and Γ_i. The requirement that the inverse rapid heat deposition problem be defined with respect to multiple scales was investigated rigorously in Ref 12. Accordingly, it was shown that the inherent filter properties of heat diffusion in metals establish that any parameterization of temperature field histories within a workpiece subject to such processes is in general insensitive to characteristics of the process occurring at the surface, i.e., the nature of the energy coupling at the surface of the structure. Data-driven inverse analysis of such processes, therefore, requires two separate data spaces. One of these consisting of data concerning the time-dependent temperature field within the volume of the structure, and the other consisting of data concerning the spatial and temporal distribution of energy at the surface, as well as, material properties of the surface (or interface) that characterize its response on relatively small space and time scales with respect to those of heat diffusion in metals. This is necessary because constraints are required on the local temporal and spatial characteristics of the energy coupling at the surface where heat deposition occurs. For application of data-driven inverse analysis to these systems, it is not the nature of the coupling between different scales that is relevant, but rather the nature of their separability for independent parameterization. This is in contrast to analysis based on direct modeling, where representation of the coupling between different scales is typically required and may result in a system whose parameterization is ill conditioned due to sensitivity issues.

At this stage, the statement of the inverse heat deposition problem as given above can be generalized to provide for the construction of a multiscale parametric representation of rapid and localized energy deposition. This generalization is represented schematically in Fig. 1 where regions of interest for determination of the temperature field are separated according

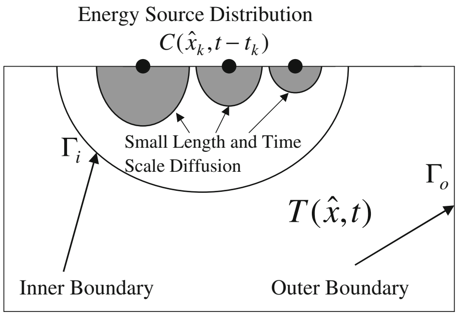

Fig. 1 Schematic representation of different regions of interest for determination of the temperature field that are separated according to the characteristic length and time scales for localized energy coupling and bulk diffusion

to the characteristic length and time scales for energy coupling at the surface and diffusion into the bulk of the system.

3. Inverse-Problem Methodology

The general inverse-problem methodology presented here is defined by the following system of equations. The time-dependent temperature field within the volume of a planar structure of finite cross section $l \times a$, upon which energy is deposited, is given by

$$T(x,y,z,t) = T_{\mathrm{A}} + \sum_{k=1}^{N_k} \sum_{n=1}^{N_t} T_k(\hat{x}, \hat{x}_k, n\Delta t) \qquad \text{(Eq 2)}$$

and

$$T(\hat{x}_n^{\mathrm{c}}, t_n^{\mathrm{c}}, \kappa) = T_n^{\mathrm{c}}, \qquad \text{(Eq 3)}$$

where the quantity T_{A} is the ambient temperature of the structure and the locations $\hat{x}_n^{\mathrm{c}}$ and temperature values T_n^{c} specify constraint conditions on the temperature field. The basis functions $T_k(\hat{x}, \hat{x}_k, n\Delta t)$ are given by

$$\begin{aligned} T_k(\hat{x}, \hat{x}_k, n\Delta t) &= \frac{C(x_k, y_k, z_k, n\Delta t)}{\sqrt{n\Delta t}} \exp\left[-\frac{(x-x_k)^2}{4\kappa(n\Delta t)}\right] \\ &\times \left\{1 + 2\sum_{m=1}^{\infty} \exp\left[-\frac{\kappa m^2 \pi^2 (n\Delta t)}{a^2}\right] \cos\left[\frac{m\pi y}{a}\right] \cos\left[\frac{m\pi y_k}{a}\right]\right\} \\ &\times \left\{1 + 2\sum_{m=1}^{\infty} \exp\left[-\frac{\kappa m^2 \pi^2 (n\Delta t)}{l^2}\right] \cos\left[\frac{m\pi z}{l}\right] \cos\left[\frac{m\pi z_k}{l}\right]\right\}, \end{aligned} \qquad \text{(Eq 4)}$$

which are solutions to the heat conduction equation for a planar structure of cross section $l \times a$ and constant diffusivity κ. The index k is for denumeration of discrete energy "deposits" at specified locations and times at the surface of the planar structure. The coefficient $C(x_k, y_k, z_k, t)$ is proportional to the energy of a given discrete deposit and is defined by

$$C(x_k, y_k, z_k, t) = \sum_{k=1}^{N_k} c(x_k, y_k, z_k) \delta(t - t_k), \qquad \text{(Eq 5)}$$

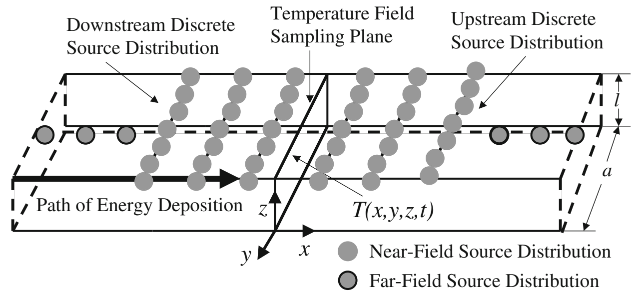

Fig. 2 Schematic representation of general algorithm structure underlying inverse-problem methodology

where $\delta(t)$ is the Dirac delta function representing the instantaneous deposition at locations (x_k, y_k, z_k) at times $t = t_k$. The speed of energy deposition, which can be a function of position on the surface of the structure, is given by

$$V_k = \frac{x_k - x_{k-1}}{t_k - t_{k-1}}. \qquad \text{(Eq 6)}$$

The formal procedure underlying the inverse method considered here entails the adjustment of the parameters $c(x_k, y_k, z_k)$ and t_k defined over the entire spatial region of the surface of the structure. This approach defines an optimization procedure where the temperature field spanning the spatial region of the sample volume is adopted as the quantity to be optimized. The constraint conditions are imposed on the temperature field spanning the bounded spatial domain of the structure by minimization of the value of the objective functions defined by

$$Z_{\mathrm{T}} = \sum_{n=1}^{N} w_n \left(T\left(\hat{x}_n^{\mathrm{c}}, t_n^{\mathrm{c}}, \kappa\right) - T_n^{\mathrm{c}}\right)^2, \qquad \text{(Eq 7)}$$

where T_n^{c} is the target temperature for position $\hat{x}_n^{\mathrm{c}} = (x_n^{\mathrm{c}}, y_n^{\mathrm{c}}, z_n^{\mathrm{c}})$.

The inverse-problem methodology defined by Eqs 2 to 7 is applied with respect to two different space and time scales. The general procedure for multiscale application of this methodology is defined according to the concepts and properties presented in the following section.

4. Concepts Underlying Inverse-Problem Methodology

The following concepts concerning the inverse-problem methodology presented here, for the analysis of processes involving rapid and localized energy deposition, are important for the understanding and application of inverse analysis to these types of processes. These concepts can be discussed with reference to Fig. 2, which provides a schematic representation of the general approach underlying the inverse-problem methodology.

(1) The temporal characteristics of the coefficients $C(x_k, y_k, z_k, t)$ defined by Eq 5 are uncorrelated with those the temperature field $T(x, y, z, t)$ spanning the region within the boundaries Γ_{o} and Γ_{i}. In fact, with respect to boundary Γ_{o}, the "coupling mechanism" for small length and

time scale diffusion of energy (see Fig. 1) within the region bounded by Γ_o and the surface of the structure represent the unknown to be determined by inverse analysis. Accordingly, information concerning the coupling of energy at the surface represents the "output" of the model system.

(2) The spatial characteristics of the coefficients $C(x_k, y_k, z_k, t)$ defined by Eq 5, i.e., the spatial distribution of the discrete-deposit strengths $c(x_k, y_k, z_k)$ (see Eq 5), are strongly correlated with of those the temperature field $T(x, y, z, t)$ spanning the region within the boundaries Γ_o and Γ_i.

(3) Inverse analysis requires a data space consisting of information concerning $C(x_k, y_k, z_k, t)$, Γ_o and Γ_i as a function of time for both the period of energy deposition and of diffusion within the structure (see Fig. 1). That is to say, information concerning these quantities represents the "input" to the model system.

(4) The naïve procedure for application of the methodology defined by Eq 2 to 7 for multiscale inverse analysis implies a computational cost that is of order $N_e \times N_s$ per discrete time step Δt_s, where N_e is the number of discrete spatial elements making up the model system, N_s is the number of discrete sources, and Δt_s is a time step that is commensurate with the characteristic time scale of rapid energy deposition at the surface. The multiscale character of rapid energy deposition, as well as the general approach defined by Eq 2 to 7, which is in terms of a basis function representation of the temperature field, provides for a range of different procedures for reduction of computational cost and improved convenience for parameter optimization.

(5) Computational cost can be reduced by calculating the temperature field only over localized regions or at a finite set of positions within the structure, which would correspond to localized sampling of the temperature field for objective function minimization with respect to the available data space. This is represented schematically in Fig. 2.

(6) Computational cost can be reduced owing to the fact that energy deposition at the surface, represented by a discrete surface distribution of sources, can be associated with separate space and time scales. Accordingly, after the time period for completion of energy deposition, the time evolution for coupling of energy at the surface into the volume of the structure can be modeled on the timescale of energy diffusion within the bulk material comprising the structure. That is to say, after the period of rapid energy deposition Δt_s, during which highly localized energy coupling occurs, system evolution can be modeled using a time step Δt_l, which is commensurate with the characteristic time scale of heat diffusion in the bulk material.

(7) Computational cost can be reduced by replacing portions of the discrete surface distribution of sources, at distances sufficiently far from the regions of the calculated temperature field, with "equivalent far-field distributions" of sources. The applicability of this procedure follows from the general nonuniqueness of local-to-far-field mappings.

(8) The multiscale characteristics of rapid energy deposition are such that the temperature field to be simulated assumes the general parameterization $T(\hat{x}, c_n(\hat{x}_n), c_f(\hat{x}_f), \Delta t_s, \Delta t_l)$, where $c_n(\hat{x}_n)$ and $c_f(\hat{x}_f)$ are near and far-field discrete source distributions, respectively, and Δt_s and Δt_l are quantities that are commensurate with the characteristic time scales of rapid energy deposition and bulk-material heat diffusion, respectively.

In what follows the concepts listed above are examined within the context prototype analyses of heat transfer occurring within structures upon whose surfaces energy is deposited both rapidly and locally.

5. Numerical Simulation and Prototype Analyses

Presented first in this section is a description of the numerical simulation adopted for generation of synthetic measurements for the purpose of constructing a prototype inverse analysis of a rapid energy deposition processes. The prototype system to be simulated is that of time-dependent rapid energy deposition at the surface of a structure of finite cross section along a linear path. The prototype measurements are the calculated temperature histories at different locations spanning a cross-sectional plane within the structure with respect to the distribution of sites of energy deposition on the surface of the structure. The model parameters for the prototype system are given in Table 1. The relative positioning of the source elements at the surface of the structure is described in Fig. 3.

For purposes of this analysis, it is assumed that the speed of energy deposition is 100 m/s and that the spatial distribution of energy deposition is uniform and observed experimentally. These conditions imply that the discrete distribution of sources is associated with a time period Δt_s for energy coupling of the entire distribution into the volume of the structure that is approximately 7.5×10^{-4} s. Accordingly, a reasonable time step Δt_l for simulation of bulk diffusion is $\Delta t = 1.0 \times 10^{-4}$ s (Table 1). The strength of each discrete source, however, is to be adjusted with respect to additional experimental data, an example of which is given by the calculated temperature fields

Table 1 Model parameters used to determine thermal fields in rapid energy deposition process

Model parameters
Material: steel
Diffusivity: $\kappa = 1.5 \times 10^{-5}$ m^2/s
Time step: $\Delta t = 1.0 \times 10^{-4}$ s
Volume element: $(\Delta l)^3$, where $\Delta l = 0.2$ mm
Cross section of structure: 50 $\Delta l \times 400$ Δl
Discrete source values: $C(\hat{x}_k, t - t_k) = 80.0$ °C m
Discrete source distribution: 15×7 elements upstream and 15×7 elements downstream of sampling plane (relative positions in Fig. 3)

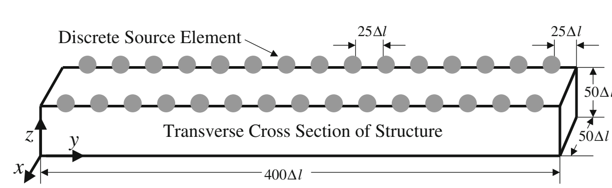

Fig. 3 Relative positions of source elements within discrete source distribution at surface of structure

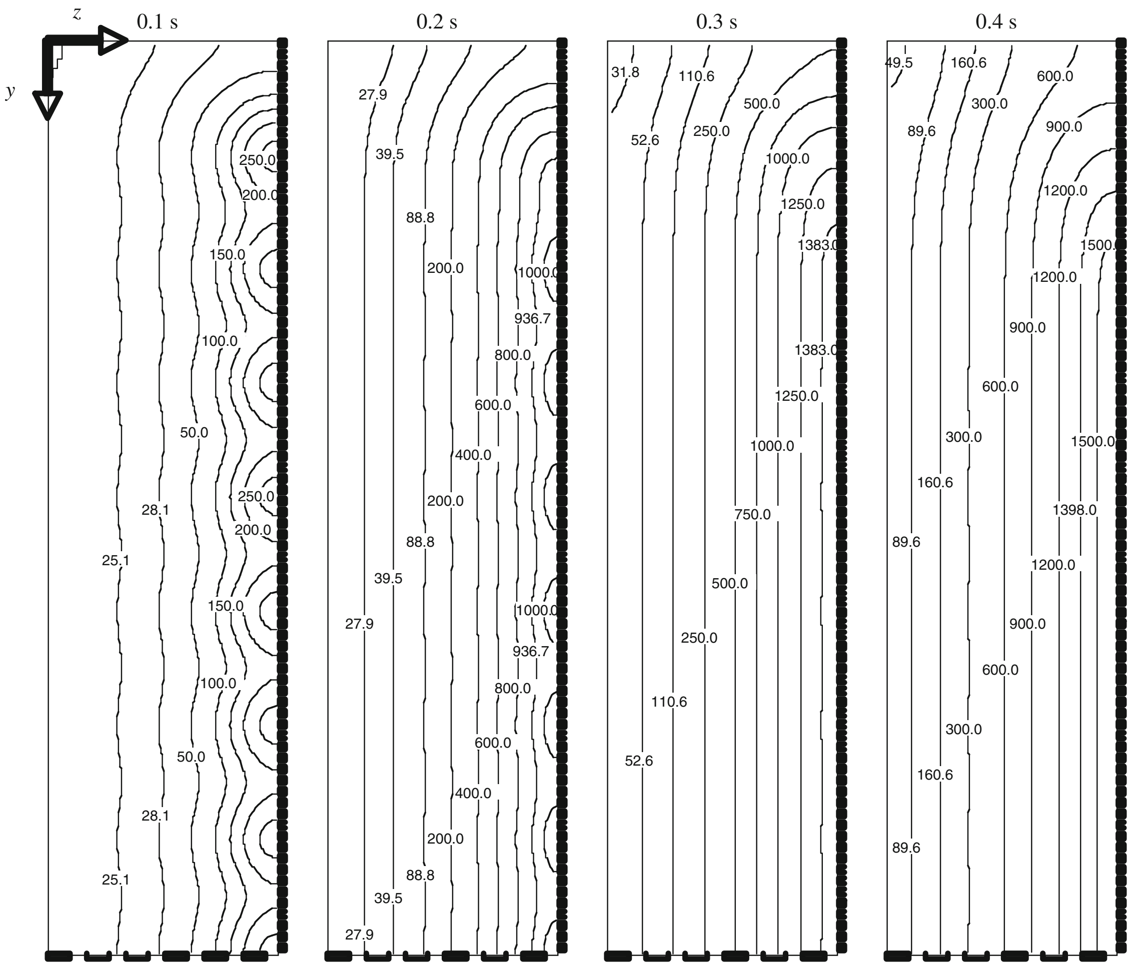

Fig. 4 Evolution of temperature field (°C) at sampling plane during time period immediately following completion of energy deposition. *Dashed* and *dotted* lines indicate location of symmetry plane and surface of energy deposition, respectively

shown in Fig. 4 to 6, where it is assumed that the ambient temperature $T_A = 25$ °C. Various aspects of the temperature fields shown in these figures that are relevant for multiscale inverse analysis of rapid energy deposition are as follows.

Shown in Fig. 4 to 6 is the time dependence of the two-dimensional temperature field over the cross section of the sampling plane (as defined by Fig. 2). The time-dependent temperature field shown in Fig. 4 is for the time period immediately following completion of energy deposition at the surface. Referring to this figure, it is noted that the discrete character of the source distribution is readily observable. It should be noted at this point, however, that the detailed spatial character of this distribution is not important, since the purpose of this source distribution is the generation of a surface Γ_i (see Fig. 1), which can be correlated with experimental data such as phase changes. Accordingly, only the total amount of energy that is coupled into the bulk volume of the material, which manifests as the experimentally observed Γ_i, is of significance. Given that the prototype material assumed for this analysis is steel, it follows that the solidus temperature is close to 1500 °C. Referring to Fig. 4, it is observed that at 0.4 s temperature values corresponding to a solidification boundary are readily observable and that any detailed spatial structure associated with the discrete nature of the source distribution has been filtered (see Ref 12 for further discussion). For the purposes of this analysis, it is assumed that the solidification boundary at approximately 1500 °C represents the experimentally observed Γ_i to be adopted as a constraint on the calculated temperature field.

The time-dependent temperature field shown in Fig. 5 is for the time period following maximum heating of the sampling plane at 0.5 s and its subsequent cooling. For this analysis, the solidification boundary at the temperature 1500 °C, which is assumed to be observed experimentally, is adopted as the constraint condition for adjustment of discrete source distribution $c\,(x_k, y_k, z_k)$ (defined in Eq 5) and thus specification of the inner boundary Γ_i.

The time-dependent temperature field shown in Fig. 6 is for the time period corresponding to onset of far-field influences on the temperature field at the sampling plane. These influences would include the shape of the outer boundary surface Γ_o, which would typically correspond to the physical boundary of the structure, and the far-field source distribution (see Fig. 2), which would result in an overall increase in temperature of the system. For the purposes of this analysis, it is assumed that temperature measurements at the physical boundary of the system, e.g., thermocouple measurements, would represent specification of the outer boundary Γ_o, and thus a constraint condition for adjustment of source element values associated with the far-field source distribution. It is significant to note that

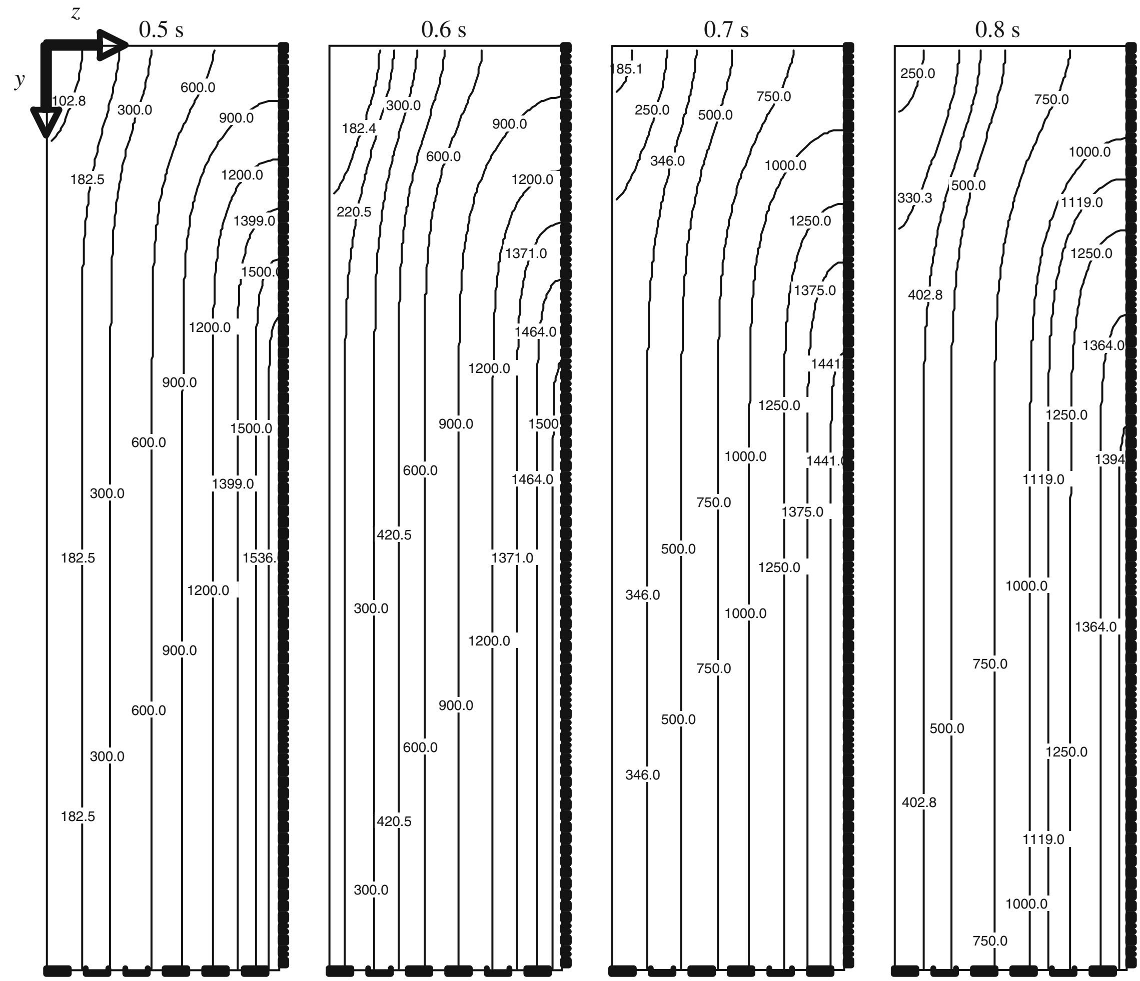

Fig. 5 Evolution of temperature field (°C) at sampling plane during time period corresponding to adjustment of temperature field, i.e., adjustment of discrete distribution c (x_k, y_k, z_k), according to experimentally observed data. *Dashed* and *dotted* lines indicate location of symmetry plane and surface of energy deposition, respectively

although the far-field source distribution would represent input information to the model system, it is not necessary to consider any details of its spatial structure owing to the inherent spatial filtering of far-field diffusion patterns. Accordingly, the far-field source distribution can be represented by means of a discrete linear source distribution such as that represented schematically in Fig. 2.

At this stage, it is instructive to review the essential aspects of the simulation described above that are relevant for multiscale inverse analysis of rapid energy deposition. First, it is noted that the procedure presented here provides for the determination of the spatial characteristics of the time-dependent diffusion pattern of energy that is coupled into the volume of a structure. Given this information, which is the result of data-driven inverse analysis, the goal is the determination of the time-dependent coupling between the rapid energy deposition process, which is assumed known, and the surface of the structure on the timescale of energy deposition. Second, given the time-dependent diffusion pattern of energy that is coupled into the volume of a structure, one is able to deduce the function $Q_{\mathrm{s}}(\hat{x}_{\mathrm{s}}, \Delta t_{\mathrm{s}})$, which is the surface distribution of energy immediately after completion of the deposition process. Third, given knowledge of rapid energy deposition process that is independent of its coupling to the surface of the structure, one is able to deduce the function $Q_{\mathrm{rdp}}(\hat{x}_{\mathrm{s}}, t)$, for $t < \Delta t_{\mathrm{s}}$, which is the time-dependent spatial distribution of energy as it occurs in free space. It is significant to note that the function $Q_{\mathrm{rdp}}(\hat{x}_{\mathrm{s}}, t)$ associated with a given rapid energy deposition process can be deduced, in principle, from data obtained from both laboratory measurements and numerical simulations based on physical models. Finally, given the functions $Q_{\mathrm{s}}(\hat{x}_{\mathrm{s}}, \Delta t_{\mathrm{s}})$ and $Q_{\mathrm{rdp}}(\hat{x}_{\mathrm{s}}, t)$, one is able to define a coefficient $\gamma(\hat{x}_{\mathrm{s}}, t)$ for the fraction of energy deposited at the surface that couples into the structure by the expression

$$\gamma(\hat{x}_{\mathrm{s}}, t) = \frac{Q_{\mathrm{s}}(\hat{x}_{\mathrm{s}}, \Delta t_{\mathrm{s}})}{Q_{\mathrm{rpd}}(\hat{x}_{\mathrm{s}}, t)}, \qquad \text{(Eq 8)}$$

where $t < \Delta t_{\mathrm{s}}$. It is significant to note that Eq 8 defines a procedure for determining the coefficient of energy coupling, in general, for processes where there does not exist a correlation between the local spatial-temporal structure of the volumetrically coupled energy source and the bulk diffusion pattern. In particular, the procedure defined by Eq 8 is independent of the size of Δt_{s}, i.e., the time scale for the total period of energy deposition. This general property establishes its applicability to the inverse analysis of rapid energy deposition.

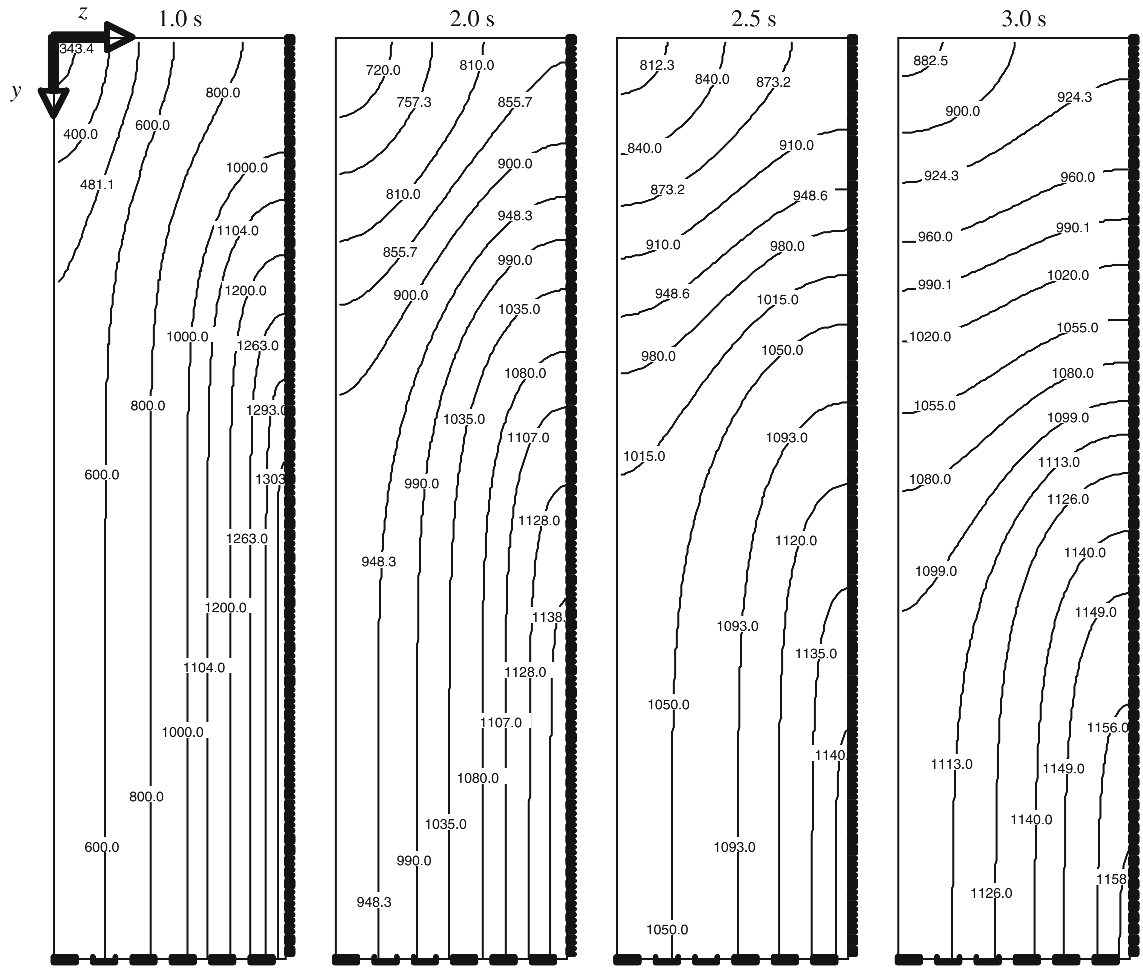

Fig. 6 Evolution of temperature field (°C) at sampling plane during time period corresponding to onset of far-field influences. *Dashed* and *dotted* lines indicate location of symmetry plane and surface of energy deposition, respectively

The purpose of the simulation given above is to demonstrate that the inherent filter properties of rapid energy deposition do not permit correlation between source structure and bulk energy diffusion. The general characteristics of source structure that do not correlate with bulk diffusion structure, however, are "independent" of the rate of energy deposition, but dependent on the coupling characteristics of the source relative to the speed of deposition. Accordingly, application of Eq 8 for inverse analysis of processes where there is rapid energy deposition can be demonstrated by consideration of a process where the rate of energy deposition is not excessively rapid relative to the time scale of bulk diffusion, but sufficiently rapid that there is weak coupling between the energy source and surface of structure. That is to say, the long-time-scale equivalent of rapid energy deposition is energy deposition characterized by relatively weak and localized coupling between source and structure. A prototype inverse analysis of such a system according to Eq 8 is now considered.

Shown in Fig. 7 is the cross section of a steel plate (21-6-9 stainless steel) of thickness 3.05 mm upon whose surface energy has been deposited by a laser beam (Diode-Pumped Continuous Wave (CW) Nd:YAG laser). The process parameters for the laser beam have been adjusted such that there is relatively weak coupling between the beam and plate surface. For this system, the model parameter values assumed are $\kappa = 5 \times 10^{-6}$ m^2/s and $T_M = 1500$ °C, which is approximately the solidus temperature for steel in general. The power and travel speed of the laser beam are 500 W and 1.905 mm/s,

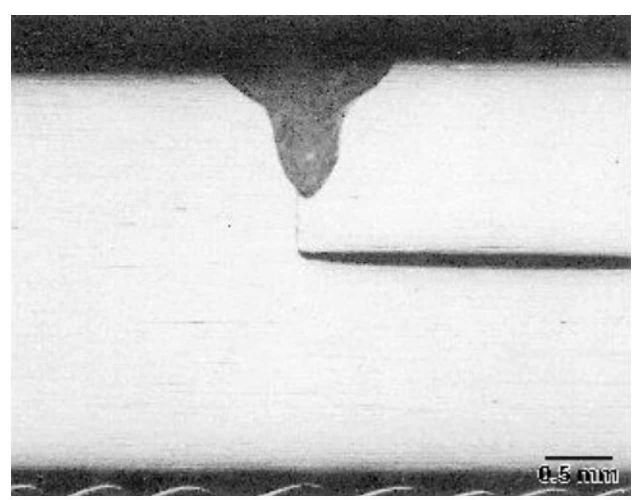

Fig. 7 Melt pool and heat-affected zone (HAZ) resulting from energy deposition from laser beam on steel plate. Beam power and welding speed are 500 W and 1.905 cm/s, respectively

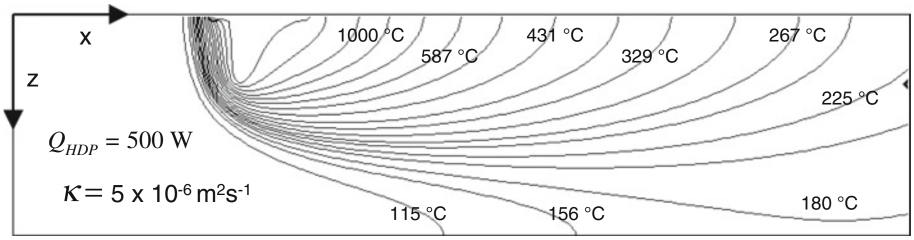

Fig. 8 Longitudinal slice of three-dimensional temperature field at midplane of melt-bead path, i.e., along *zx*-plane at $y = 0$

Table 2 Temperature field constraint conditions at positions (y_c, z_c) on transverse cross section at solidification boundary

y_c, mm	z_c, mm
0.6875	0.0
0.5	0.125
0.25	0.313
0.375	0.5
0.125	0.813
0.0	1.0

respectively. Accordingly, $Q_{\mathrm{rdp}}(\hat{x}_{\mathrm{s}}, t)$ defined in Eq 8 has a constant value of 262.5 mm/s. The constraints on the calculated temperature field defined according to Eq 3 are given in Table 2.

Shown in Fig. 8 is a two-dimensional slice of the three-dimensional temperature field calculated according to the procedure defined by Eq 2 through 7. This temperature field determines $Q_{\mathrm{rdp}}(\hat{x}_{\mathrm{s}}, t)$. That is to say, the volume integral of this temperature field, weighted by the temperature-dependent density and volume-specific heat capacity, represents a specification of the function $Q_{\mathrm{s}}(\hat{x}_{\mathrm{s}}, \Delta t_{\mathrm{s}})$. It is significant to note that the exact form of this weighting still remains an issue to be addressed in that the localized structure of volumetric coupling of the energy source at the surface is assumed not known exactly. Reasonable estimates of $Q_{\mathrm{s}}(\hat{x}_{\mathrm{s}}, \Delta t_{\mathrm{s}})$, however, based on volumetric averages are certainly well defined for providing good quantitative estimates of $\gamma(\hat{x}_{\mathrm{s}}, t)$. Further analysis concerning procedures for the construction of $Q_{\mathrm{s}}(\hat{x}_{\mathrm{s}}, \Delta t_{\mathrm{s}})$ is required.

6. Conclusion

A general approach has been presented for multiscale inverse analysis of rapid and localized energy deposition where the characteristic time and space scales for energy deposition at the surface of a structure are significantly smaller than those for energy diffusion into its bulk volume. A characterization of the nature of the coupling between these different scales is achieved, in principle, by means of the determination of a coefficient $\gamma(\hat{x}_{\mathrm{s}}, t)$ that represents the fraction of energy deposited at the surface that couples into the volume of the structure.

Acknowledgments

The authors acknowledge the support by the Office of Naval Research (ONR) and the Naval Research Laboratory (NRL) internal core program.

References

1. M.N. Ozisik and H.R.B. Orlande, *Inverse Heat Transfer, Fundamentals and Applications*, Taylor and Francis, New York, 2000
2. K. Kurpisz and A.J. Nowak, *Inverse Thermal Problems*, Computational Mechanics Publications, Boston, USA, 1995
3. O.M. Alifanov, *Inverse Heat Transfer Problems*, Springer, Berlin, 1994
4. J.V. Beck, B. Blackwell, and C.R. St. Clair, *Inverse Heat Conduction: Ill-Posed Problems*, Wiley Interscience, New York, 1985
5. V.A. Karkhin, V.V. Plochikhine, A.S. Ilyin, and H.W. Bergmann, Inverse Modelling of Fusion Welding Process, *Mathematical Modelling of Weld Phenomena 6*, H. Cerjak, Ed., Maney Publishing, London, 2002, p 1017–1042
6. S.G. Lambrakos and J.G. Michopoulos, Algorithms for Inverse Analysis of Heat Deposition Processes, *Mathematical Modelling of Weld Phenomena*, Vol 8, Verlag der Technischen Universite Graz, Austria, 2007, p 847
7. J. Michopoulos and S. Lambrakos, On the Fundamental Tautology of Validating Data-Driven Models and Simulations, *International Conference on Computational Science*, Vol 2, 2005, p 738–745
8. J.G. Michopoulos and S.G. Lambrakos, Underling Issues Associated with Validation and Verification of Dynamic Data Driven Simulation, *Proceedings of the 2006 Winter Simulation Conference*, L.F. Perrone, F.P. Wieland, J. Liu, B.G. Lawson, D.M. Nicol, and R.M. Fujimoto, Ed., CD-ROM, ISBN 1-4244-0501-7, IEEE Catalog N. 06CH37826
9. A. Kirsch, *An Introduction to the Mathematical Theory of Inverse Problems*, Springer Verlag, New York, 1996
10. S.G. Lambrakos and J.O. Milewski, Analysis of Processes Involving Heat Deposition using Constrained Optimization, *Sci. Technol. Weld. Join.*, 2002, **7**(3), p 137
11. J. Xie and J. Zou, Numerical Reconstruction of Heat Fluxes, *SIAM J. Numer. Anal.*, 2005, **43**(4), p 1504–1535
12. S.G. Lambrakos and J.G. Michopoulos, Multiscale Implications of the Inverse Rapid-Energy Deposition Problem, *Int. J. Multiscale Comput. Eng.*, 2009, **7**, p 41–53